Three Dynamic Problems in Robot Force Control

Steven D. Eppinger, *Member, IEEE,* and Warren P. Seering

Abstract—**The dynamic characteristics of a mechanical system constrain system performance. Three dynamic characteristics of robot systems are discussed here: rigid-body bandwidth, dynamically noncolocated flexible modes, and dynamically colocated flexible modes. All of these combine to limit the closed-loop bandwidth achievable in the individual joint control loops of the robot. They play a particularly important role in establishing performance limits for robots under force control.**

I. Introduction

ROBOTS will become a more important component of automated manufacturing systems when their speed and capabilities are increased [11], [14]. Most industrial robots in use today are simple position-controlled manipulators that use joint (or actuator) position feedback to close the control loops. Their applications are limited to operations where the manipulator uses little or no sensed information from its environment. Position control is useful in tasks where the robot is not constrained by objects in the workspace. Examples of successful industrial applications of position control include spray painting and pick-and-place tasks.

In many automated manufacturing processes, the robot is required to interact with its environment in a more controlled manner, while that environment is only imprecisely known. In mechanical assembly, for example, the manipulator must mate parts whose position, orientation, size, and shape are somewhat uncertain. A great deal of effort is now being placed on the development of new sensor systems for use in industrial robot applications. Sensing and computation, combined with superior robot/control system design, can greatly increase the potential of industrial robots.

Robot force control is the term used to describe control schemes where measurements of the interaction forces are used to alter the trajectory commands given to the joint servos of a robot. (The term compliant motion control is also used to describe these schemes.) Many force control algorithms have been developed [13], and many performance problems have been investigated [1], [4], [5], [10].

Dynamic performance is limited in all machine systems; we cannot increase robot response without bound. Achievable performance depends on the quality of both the mechanical system design and the employed controller. Performance limitations come about in a variety of forms. For example, a robot system under joint position control may not be able to track the programmed trajectory. A robot under end point force control may exhibit a violent chatter upon contact with the environment. To avoid these dynamic problems, control gains must typically be reduced until stable behavior is obtained. In some cases, the control system is primarily to blame for the instability. However, in most cases, the dynamic characteristics of the robot system contribute significantly to limiting the closed-loop performance. Unless this dynamic behavior is fully understood, one cannot predict the effects of closed-loop control.

This article examines three dynamic effects of importance in robot control. These are:

- rigid-body bandwidth,
- dynamically noncolocated modes, and
- dynamically colocated modes.

The rigid-body bandwidth represents the performance of the system in the absence of all flexibility. There are two basic types of flexibility (or compliance) in robot systems, and these are classified by the location of the compliant elements. Compliance between the actuator and sensor gives rise to dynamically noncolocated modes, in which the actuator and sensor can vibrate out of phase. Flexibility that is not between the actuator and sensor gives rise to dynamically colocated modes, in which the actuator and sensor remain in phase.

Our goal here is to describe the impact of these dynamic effects on robot force control performance. We will focus on force control, though the conclusions apply for certain other control strategies. We will discuss performance by building mathematical models of systems representing simple robots and analyzing the actuator-to-sensor transfer functions for these systems. Some laboratory data will then be presented to illustrate the presence of comparable dynamic effects in complex robotic systems. Finally, the implications for robot system design will be discussed.

II. Modeling Machine Performance

In this paper, we will not employ models of multiaxis robots. Such models are essential for properly designing controllers for actual robotic systems. However, it is possible to illustrate and evaluate the impact of typical robot dynamic effects on models of single robot axes. We will do so for simplicity; it can easily be shown that the effects and consequences generalize to multilink systems. A great deal can be learned about robot performance under force control by considering the linear, higher order behavior of a single axis coupled with

Manuscript received September 6, 1991; revised May 19, 1992. The research described in this paper was performed at the Massachusetts Institute of Technology Artificial Intelligence Laboratory, which is supported in part by the Office of Naval Research University Research Initiative Program under Office of Naval Research Contract N00014-86-K-0685, and in part by the Advanced Research Projects Agency of the Department of Defense under Office of Naval Research Contract N00014-85-K-0124. This work was also supported in part by the TRW Foundation. This paper was presented at the IEEE International Conference on Robotics and Automation, Scottsdale, AZ, May 1989.

The authors are with the Massachusetts Institute of Technology, Cambridge, MA 02139.

IEEE Log Number 9203665.

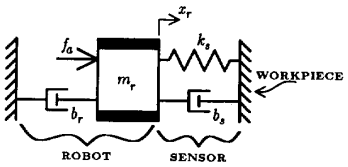

Fig. 1. Rigid-body robot model with rigid workpiece.

a workpiece. We will begin by discussing a simple one-mass model, representing the rigid-body behavior of one axis. We include the actuator dynamics and couple the actuator model to the rigid robot model. Next, various forms of flexibility are added to the rigid-body model. We consider the transmission, link, base, and workpiece compliance.

Most of the models developed here show the robot in contact with either a rigid or a dynamic workpiece. This emphasis on constrained robot dynamics is meant to help us think in terms of the coupled behavior of the robot under force control. These models can be used to evaluate unconstrained (position-control) performance if the components representing the force sensor and workpiece are eliminated. The models presented here are lumped-parameter dynamic models. In real systems, however, the physical properties may be nonlinear and/or distributed throughout the machine. Nevertheless, the lumped-parameter approximation is very often a good one, and it is well suited to our purposes of developing useful insight about how systems behave.

We will use two linear system analysis tools, the bode plot and the root-locus plot; however, we will discuss the analysis without explicitly giving numerical parameters for the models. The resulting plot shapes are generated for typical robot parameters (those of a Cartesian system in our lab) and are chosen because they are representative of typical machine systems. The parameters were obtained through reference to a detailed model of the chosen system, which has been described in [6].

III. Rigid-Body Bandwidth

Let us consider one robot degree of freedom (a single axis, link, or joint) and its interaction with the environment. Fig. 1 shows the effective inertia (total moving mass) of the axis as m_r and the effective viscous damping to ground as b_r. For force control, we model the force sensor as a linear spring, with stiffness k_s and damping b_s, between the robot and the workpiece. For now, we model the workpiece as rigid, or ground. The actuator effort f_a is the system input, and the outputs are the robot position x_r and the force across the sensor $f_s = k_s x_r$.

Without explicitly including an actuator in our robot model, we would implicitly assume that the actuator response is perfect. In reality, of course, the actuator response is limited. All actuators have both bandwidth and effort limitations. In addition, when the actuator is coupled to a load, the load characteristics can affect the actuator performance. We construct a typical bandwidth-limited actuator model and couple it to the robot model. While nonlinear saturation effects are often significant, we restrict our analysis here to this linear

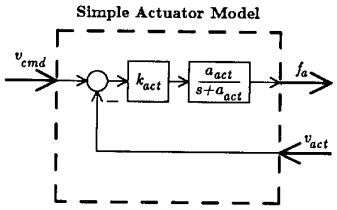

Fig. 2. Generic bandwidth-limited actuator model.

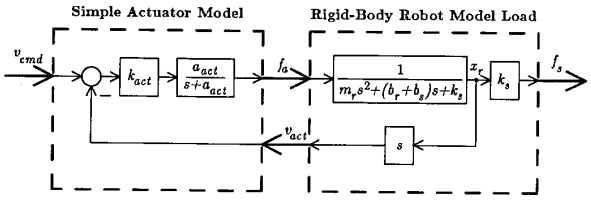

Fig. 3. Actuator model coupled to the rigid-body robot model.

example. A sketch of a simple actuator model is shown in Fig. 2. The input to this model is the actuator velocity command. As modeled, the actuator represents a voltage amplifier. For more powerful amplifiers, higher actuator bandwidths should be modeled. (If the system employs a high-bandwidth current amplifier, the actuator model need not be employed except as desired to represent saturation conditions.)

Now we couple the rigid robot model to the simple actuator model, as shown in Fig. 3, and evaluate the coupled performance. The open-loop transfer function, from input actuator command to output sensed force, becomes third order. The coupled system's open-loop bode plot is shown in Fig. 4, and it displays the phase lags associated with the actuator and the robot inertia. For feedback of the sensed force, the explicit-force-control root-locus plot is shown in Fig. 5. The imperfect actuator clearly affects the rigid-body robot model response, making the closed-loop system unstable for high gains. Increasing the actuator bandwidth increases the range of gains for which the system is stable. In the absence of actuator limitations, the model predicts stability for all gains and all values of model parameters. It should be noted that operating the system in Fig. 3 under position control would not improve its stability characteristics.

IV. Modeling Machine Flexibility

A rigid-body model is severely limited in its ability to represent real machine systems, which always include some forms of flexibility. Examples of sources of flexibility in robot systems are: gear tooth bending, bearing mount compliance, link bending or torsion, mounting base compliance, bending of axis guides or ways, force sensor compliance, grasp compliance, and workpiece compliance. Note that some of these flexible elements are physically located between the actuator and sensor, while others are not. We find this distinction to be important since the two cases produce different effects on dynamic performance.

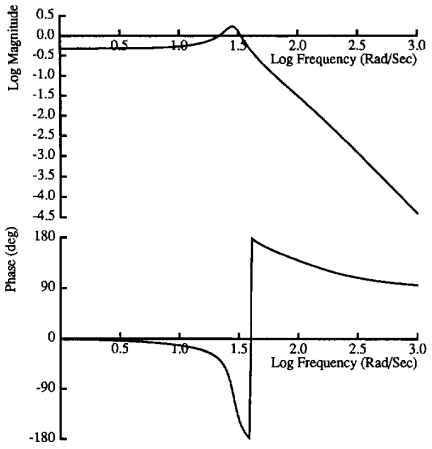

Fig. 4. Bode plot for the rigid-body coupled model.

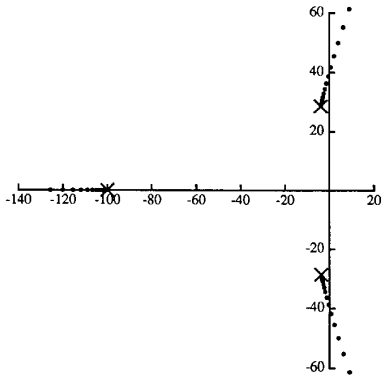

Fig. 5. Root-locus plot for the rigid-body coupled model.

V. Dynamically Noncolocated Modes

As an example of noncolocated dynamics, we will consider transmission and/or link flexibility. The transmission and link dynamically couple the actuator to the end-point. In the model discussed previously, we have assumed that the actuator velocity is the same as the end-point velocity. In fact, with any flexibility in either the transmission or the link, there will be frequencies above which the actuator and end-point velocities will not only be different, but will be completely out of phase. Since both transmission compliance and link or axis compliance can give rise to this same dynamic effect, we consider them collectively.

We can include the compliance of the transmission or link by adding another lumped mass to the rigid-body robot model above and placing a spring between the two masses, as shown in Fig. 6. The robot itself is now represented by the two masses, m_{r1} and m_{r2}, and the flexibility between them is given by k_{rf} and b_{rf}. For now, we will use the simple sensor and workpiece model, and for simplicity we will analyze the robot model with a perfect actuator model.

If the stiffness of the transmission is low, as in a harmonic drive [8] or as with flexible tendons [9], then the robot compliance k_{rf} would reflect this transmission flexibility. If

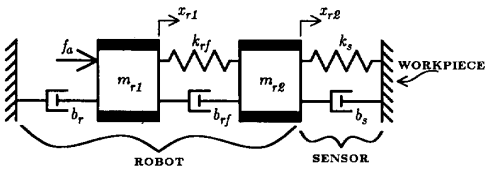

Fig. 6. Robot model with transmission or link flexibility.

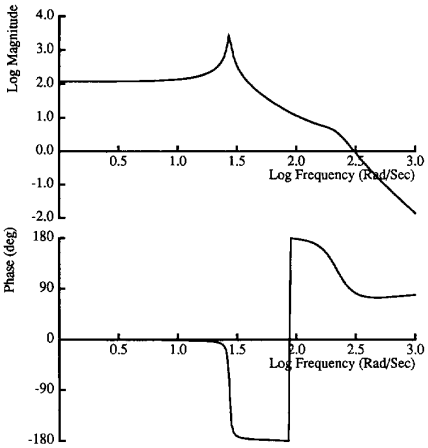

Fig. 7. Bode plot for the flexible robot model.

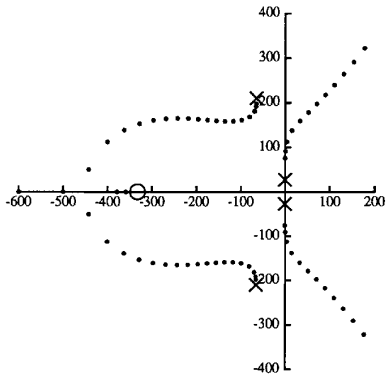

Fig. 8. Root locus plot for the flexible robot model.

the link itself is flexible [3], then the robot compliance reflects this link flexibility. The open-loop bode plot, Fig. 7, and the root-locus plot, Fig. 8, demonstrate the effect of adding the robot flexibility to the rigid-body robot model. The bode plot shows that a sharp phase drop occurs at the frequency of the flexible mode. The root locus plot shows that, for high gains, the system has closed-loop roots in the right half of the s plane. We refer to this effect as *noncolocation*, first discussed by Gevarter [7] in the context of controlling flexible vehicles. Gevarter showed that if an actuator and sensor are physically located at different points on a flexible structure, then there will be unstable modes in the closed-loop system. He also showed that *colocation* does not guarantee stable closed-loop control. (Even if an actuator and sensor are physically colocated, there

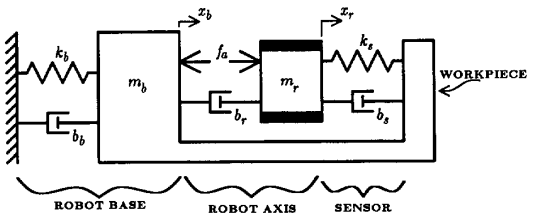

Fig. 9. A robot model including base flexibility.

can still be modes in which the actuator output and the sensor signal are out of phase, while for the rigid-body mode, they are in phase. It depends upon what is being measured and where the actuator/sensor pair is placed on the structure.)

Robot flexibility then is certainly one possible cause of robot force control instability. Note that, under traditional position control, the model in Fig. 6 predicts system stability at all gains. This result implies that for a representative system the performance limit for force control is lower than that for position control given some degree of transmission or link flexibility.

VI. Dynamically Colocated Modes

As examples of the other major class of robot compliance, we consider two forms of flexibility that give rise to modes in which the actuator and sensor do not necessarily vibrate opposite in phase. These forms are those of base dynamics and workpiece dynamics.

A robot can be quite a massive machine tool, and the base on which it is mounted is never perfectly rigid. In fact, the base compliance can and often does give rise to the lowest frequency mode of vibration observed in the robot structure. This is so for the MIT Precision Assembly Robot, for which the lowest-frequency mode is the "base mode," at approximately 12 Hz [6].

Fig. 9 shows a robot model in which we include base dynamics. The robot has a compliant base, and this base also supports the workpiece. In the base dynamics model, m_b represents the moving mass of the base, while k_b and b_b give its stiffness and damping. The actuator effort is applied to both the base and the robot. For this example, we use the simple rigid-body robot model from above to represent the arm and sensor. The workpiece is considered to be a rigid part of the base. This configuration best describes the setup of many Cartesian robots for which the workpiece is generally mounted to the robot base plate.

The bode and root locus plots for the base dynamics model are shown in Figs. 10 and 11. These plots demonstrate very clearly how this type of structural flexibility differs from the link flexibility considered in the previous section. The bode phase plot shows a sharp lag in phase followed quickly by phase lead. This behavior is typical of structural modes (with low damping) and is explained by the root locus plot, which shows that a pair of poles is very near a pair of zeros all of which are contributed by the base dynamics. As the base damping b_b is increased, the poles and zeros move away

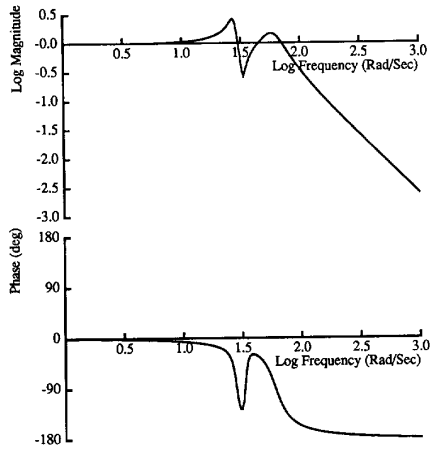

Fig. 10. Bode plot for the base flexibility model.

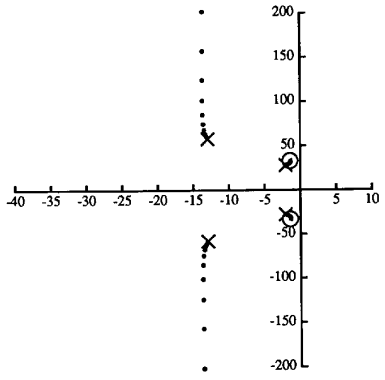

Fig. 11. Root locus plots for the base flexibility model.

from the imaginary axis and have less effect on the response. Increasing the damping in this way may be difficult but can be quite beneficial under certain conditions.

In contrast with the link and transmission compliance, the base compliance is generally less detrimental to the bandwidth of the closed-loop system. The phase dip contributed by the base dynamics does not cause instability if the rigid-body system has sufficient phase margin to keep the total phase above $-180°$ throughout the frequency range of interest. If the base mode is sufficiently damped, then the pair of poles will lie very close to the pair of zeros, minimizing the depth of the dip in phase. We call the base mode *dynamically colocated*, since the vibrations of the base do not cause the actuator and sensor to vibrate opposite in phase.

So far, we have modeled the environment as a rigid "wall." This is thought by some to be the worst-case condition for robots performing tasks under force control. (Colgate [4] has shown that, for some robot systems, a pure mass or linear spring can be the most destabilizing environment.) Now we will model the task as a second-order lumped-mass system, and investigate how these dynamics affect the stability of robot force control.

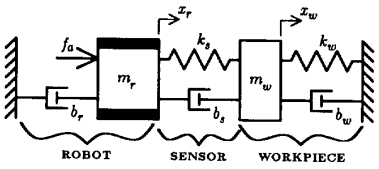

Fig. 12. Robot model including workpiece dynamics.

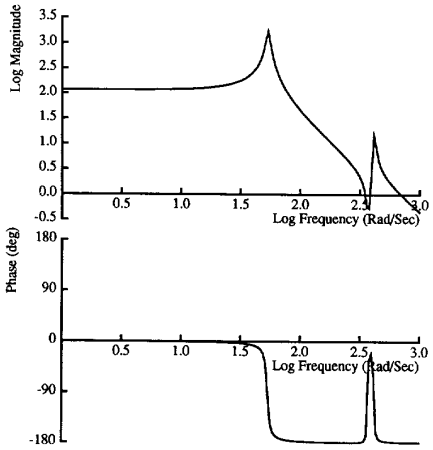

Fig. 13. Bode plot for the workpiece model.

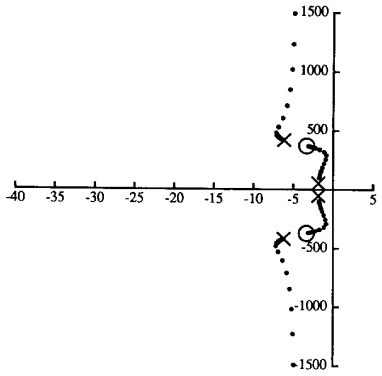

Fig. 14. Root locus plot for the workpiece model.

Fig. 12 shows the rigid-body robot model augmented with a dynamic workpiece. The workpiece has mass m_w, stiffness k_w, and damping b_w. The robot has only rigid-body dynamics, and no vibrational modes. The force sensor, with stiffness k_s, couples the robot to the workpiece.

The bode and root locus plots are shown in Figs. 13 and 14. The second-order workpiece dynamics contribute a pair of poles and a pair of zeros. This gives a phase dip to the bode plot, just like the base dynamics did. Adding more damping to the workpiece (increasing b_w) moves the pair of poles away from the imaginary axis and toward the pair of zeros, so they almost cancel. Increasing the workpiece stiffness k_w makes the workpiece poles faster, moving them away from the origin in the vertical direction.

The mode introduced by the workpiece dynamics is also dynamically colocated. That is, just like the base dynamics, the workpiece dynamics do not contribute to the actuator-to-end-point out-of-phase response. In fact, for the rigid-body robot model shown, the workpiece dynamics affect stability only in a frequency range near the resonance represented by the corresponding poles. If phase margin over the rest of the frequency range is adequate and the modal damping sufficient, the introduction of workpiece dynamics will not seriously affect stability despite the fact that these dynamics introduce poles that move vertically away from the origin as workpiece stiffness is increased. This dynamic contribution is in fact quite similar to the contribution of a second-order lead filter.

It cannot be said though that the dynamics of colocated modes are not important. The constraints mentioned above, that the phase margin be adequate over the rest of the frequency range and that damping be sufficient, may not be met for typical machines as illustrated in the next section.

VII. Experimental Data

Modeling machine performance is very important for developing an intuitive understanding of how systems behave. In addition, we should test this intuition and our models by comparing them to actual machine performance. We need data against which to judge the validity of the mathematical models, and if our models are wrong, we can create new models with the right effects included. The data presented here illustrate the issues we have discussed.

These experimental data are taken on the MIT Precision Assembly Robot, designed and built in the MIT Artificial Intelligence Laboratory [12]. The data we desire are transfer functions from the individual axis servo commands to various sensor outputs. The input given to the system is band-limited white noise generated by a structural dynamics analyzer. Various outputs are measured in the tests, and the analyzer compares the frequency components of the input and output signals, then calculates a transfer function (TF) for plotting. To understand the behavior of the robot arm itself, we send the white noise input to the velocity command voltage at the amplifier. We measure the following three outputs:

1) robot acceleration measured at the motor (colocated TF),
2) robot acceleration measured at the end-point (noncolocated TF), and
3) sensed contact force measured at the tip (noncolocated TF).

The acceleration measurements are made for the robot *not in contact* with the environment. The colocated and noncolocated transfer functions help explain the difference in the achievable bandwidths of colocated joint position control and noncolocated end-point force control. The system is the same for both tests; only the position of the accelerometer is changed. The transfer functions shown in Figs. 15 and 16 represent the open-loop arm response for the robot in free space, unattached from the workpiece. Fig. 15 shows the colocated transfer function with the accelerometer at the motor, while Fig. 16 shows the noncolocated transfer function from the motor to the robot end-point acceleration.

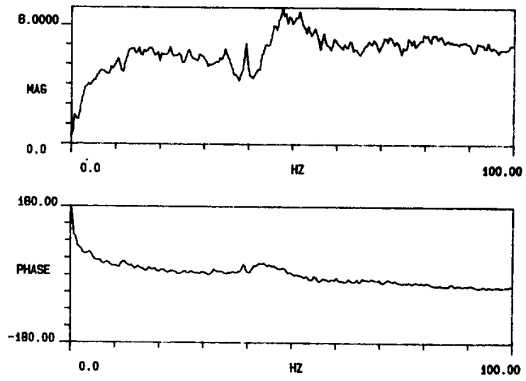

Fig. 15. Measured colocated acceleration transfer function.

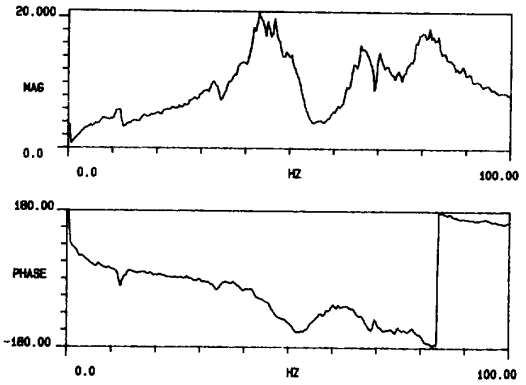

Fig. 16. Measured noncolocated acceleration transfer function.

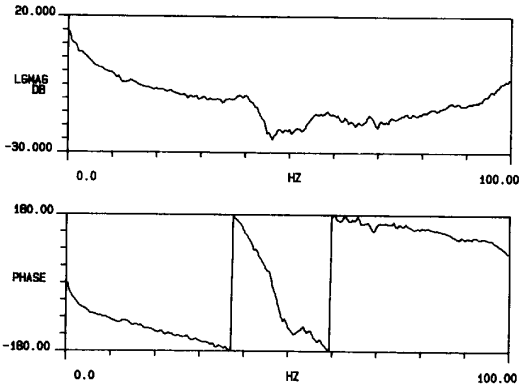

Fig. 17. Measured noncolocated force transfer function.

The contact force transfer function is measured with the end-point in contact with a dynamic workpiece. (Actually, the end-point must be clamped to the workpiece to maintain contact since the noise signal has no offset to give a bias force.) Since the force measurement is the normal output of the force sensor strain gage amplifier circuit, the transfer function from the motor input to the force sensor output represents the open-loop plant for the force control system. The force transfer function measurement is shown in Fig. 17.

It is interesting to note a few features of the robot system frequency response. The open-loop colocated and noncolocated transfer functions differ greatly. Both measurements were made on the same system; only the accelerometer placement differed. Therefore, these transfer functions have the same characteristic equation and different numerator dynamics. The noncolocated transfer function shows system resonances at 12, 38, 44, 67, and 77 Hz. The colocated transfer function does not show these resonant frequencies as clearly.

More importantly, the two acceleration transfer functions display the open-loop phase crossover frequencies for colocated (joint) and noncolocated (end-point) position control. We cannot infer the force control bandwidth from these measurements because they were recorded with the robot unattached from the environment. Since these are acceleration transfer functions, we should measure the phase margin for these plots from 0° instead of from −180°. (The position transfer functions would be shifted by 180° in phase.) Furthermore, since the robot is unattached in these experiments, there is a rigid-body motion mode in the acceleration transfer functions, giving a sharp drop in phase at low frequency. The colocated transfer function shows that the phase drops below 0° at 50 Hz, while the noncolocated transfer function dips below 0° from 11 to 13 Hz, then crosses finally at 28 Hz. We can see why the system with colocated feedback would be able to achieve greater closed-loop bandwidth. The noncolocated system shows two particular problems for end-point position control. At 12 Hz, the system loses its phase margin due to the phase dip from the colocated base mode coupled with insufficient phase margin in the contiguous region (this is the condition to which we alluded in the previous section). Even in the absence of the 12-Hz base mode, at 28 Hz the system would drop below 0° anyway as a result of the influence of the first noncolocated mode. Colocated control is simply more stable. Even though the colocated system has all of the same poles, their phase effects are largely canceled, and the colocated system has less phase lag.

The force transfer function (Fig. 17), which also measures a noncolocated situation but now with the robot attached to the workpiece, is equally interesting. It too shows the system resonances much less than the unattached noncolocated acceleration transfer function. This time, we cannot attribute this exclusively to changed numerator dynamics. The poles have actually moved because the robot is now coupled to the environment. Since the workpiece is quite stiff, it is reasonable to assume that some of the lower resonances have moved up in frequency. (The base mode is not likely to have changed much though.) The phase crossover frequency is 37 Hz.

VIII. Conclusion: A Recommendation for Robot Designers

There are many features of a machine design that determine the achievable closed-loop bandwidth for the system. Fig. 18 shows a hypothetical open-loop bode phase plot for a machine system or a robot. This phase plot has three important features: the rigid-body rolloff, a low-frequency colocated mode, and a higher frequency noncolocated mode. Each of these three

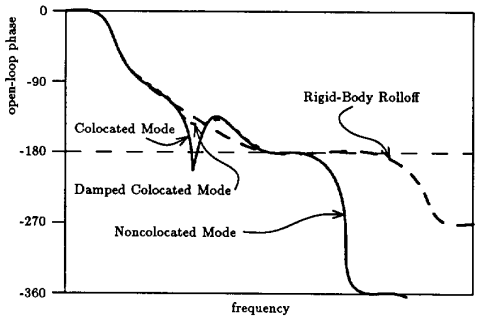

Fig. 18. Three dynamic problems in machine control.

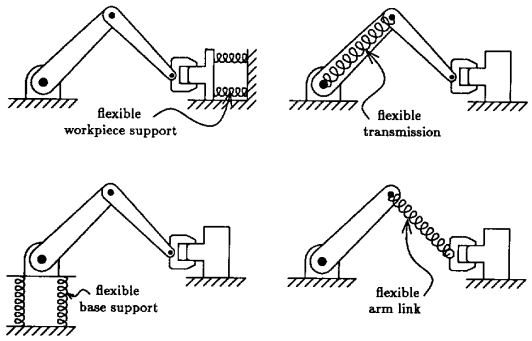

Fig. 19. Types of robot flexibility.

dynamic forms can contribute to or entirely determine the achievable bandwidth.

The rigid-body model coupled with the actuator dynamics generally has at least three more poles than zeros (two from the rigid axis and one from the actuator dynamics). This situation causes the open-loop phase to drop below $-180°$ as shown in the dashed line of Fig. 18. So even in the absence of flexibility, there is a phase crossover.

If there are dynamically colocated modes at frequencies below that of the rigid-body crossover, then these may further limit the bandwidth. Underdamped base or workpiece dynamics can give a pair of poles and a pair of zeros lying together near the imaginary axis, which can cause a sharp phase dip of 50° or more at that frequency. This dip may be enough to push the total phase below $-180°$. If the colocated mode occurs at a very low frequency, where there is greater phase margin, then the system may retain stability. If a low-frequency colocated mode is very well damped, the phase dip will be greatly diminished. Adding damping to the low-frequency modes of this type is an interesting design solution.

Dynamically noncolocated modes, such as those contributed by arm or transmission flexibility, come with more poles than zeros. These poles add phase lag and can give 180° of phase shift. The frequency of the lowest dynamically noncolocated mode is a fundamental performance limitation for conventional PD controllers.

Throughout the detailing phase, the designer is faced with decisions like: "How thick shall I specify this wall?" and "Where should I place this support?" Machine designers basically understand the tradeoffs involving mass and stiffness. They know that adding stiffness raises the resonant frequencies, which somehow helps performance, but that this stiffness can increase the moving mass, which certainly slows the machine. While designers do generally understand the rigid-body motion problem, they do not usually know about the effects of the various flexible modes. Designers need to understand enough about structural dynamics to "design the mode shapes."

Fig. 19 illustrates the different types of robot flexibility that we have discussed. Transmission and link flexibility result in noncolocated control modes in which the actuator and sensor move apart (out of phase); these will limit the achievable bandwidth. The base and workpiece dynamics contribute dynamically colocated modes, which do not necessarily adversely affect the system performance though for many cases they may. There is a third type of flexible mode, one in which there is not any relative motion between the actuator and sensor (a mode in an orthogonal direction, for example), and these modes are unimportant for this discussion.

The frequency of the lowest mode in which the actuator and sensor move opposite in phase (from their phase relation during rigid-body motion) represents a fundamental performance limitation. All of the other modes tend to be less important. The designer must pay particular attention to increasing the frequency of these dynamically noncolocated flexible modes. Every element between every actuator/sensor pair should be designed with high stiffness in mind. It is difficult to do this without increasing the effective moving mass of the axis; however, the resonance only needs to be increased beyond the open-loop phase crossover of the rigid-body model. The system designer should develop a dynamic performance model as part of the machine design process. A rigid-body model of the proposed system can be analyzed before the actuator and transmission specifications are finalized. The effective stiffness and inertia for each suspected flexible mode can also be estimated in the detailed design stage in order to keep tabs on the resonant frequencies of the machine. Methods for doing this are discussed in books on stress calculation and structural analysis [2]. Finally, these estimates can be used as parameters for performance models like those presented here. There are many methods for developing complex structural dynamics models. However, it is generally not straightforward to derive transfer functions from these models, so reduced-order models need to be chosen carefully.

REFERENCES

[1] C. H. An and J. M. Hollerbach, "Dynamic stability issues in force control of manipulators," in *Proc. IEEE Int. Conf. Robotics Automat.*, Apr. 1987, pp. 890–896.

[2] R. D. Blevins, *Formulas for Natural Frequency and Mode Shape*. New York: Van Nostrand Reinhold, 1979.

[3] R. H. Cannon and E. Schmitz, "Initial experiments on the end-point control of a flexible one-link robot," *Int. J. Robotics Res.*, vol. 3, no. 3, pp. 62–75, Fall 1984.

[4] J. E. Colgate and N. Hogan, "Robust control of manipulator interactive behavior," in *Modeling and Control of Robotic Manipulators and Manu-*

facturing Processes, R. Shoureshi, K. Youcef-Toumi, and H. Kazerooni, Eds. New York: ASME, 1987.
[5] S. D. Eppinger and W. P. Seering, "Understanding bandwidth limitations in robot force control," *IEEE Int. Conf. Robotics Automat.*, Apr. 1987, pp. 904–909.
[6] A. Garcia-Reynoso and W. P. Seering, "Modeling the vibration of systems whose configurations can vary," *ASME J. Mechanisms, Transmissions, Automat. Design*, pp. 19–24, Mar. 1989.
[7] W. B. Gevarter, "Basic relations for control of flexible vehicles," *AIAA J.*, vol. 8, no. 4, pp. 666–672, Apr. 1970.
[8] M. C. Good, L. M. Sweet, and K. L. Strobel, "Dynamic models for control system design of integrated robot and drive systems," *ASME J. Dynam. Syst. Meas. Contr.*, pp. 53–59, Mar. 1985.
[9] M. G. Hollars and R. H. Cannon, "Initial experiments on the end-point control of a two-link manipulator with flexible tendons," presented at ASME Winter Ann. Meeting, Nov. 1985.
[10] A. Sharon, N. Hogan, and D. E. Hardt, "High bandwidth force regulation and inertia reduction using a macro/micro manipulator system," in *Proc. IEEE Int. Conf. Robotics Automat.*, Apr. 1988, pp. 126–132.
[11] D. Tesar, Thirty-year forecast: The concept of a fifth generation of robotics—The super robot," *ASME Manufact. Rev.*, vol. 2, no. 1, pp. 16–25, Mar. 1989.
[12] E. Vaaler and W. P. Seering, "Design of a Cartesian robot," in *Robotics and Manufacturing Automation*, M. Donath and M. Leu, Eds. New York: ASME, 1985, pp. 163–168.
[13] D. E. Whitney, "Historical perspective and state of the art in robot force control," in *Proc. IEEE Int. Conf. Robotics Automat.*, Mar. 1985.
[14] ——, "Real robots don't need jigs," in *Proc. IEEE Int. Conf. Robotics Automat.*, Mar. 1986, pp. 746–752.

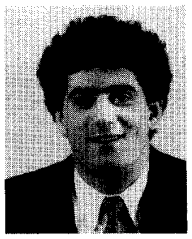

Steven D. Eppinger (S'86–M'88) receved the S.B., S.M., and Sc.D. degrees from the Department of Mechanical Engineering, Massachusetts Institute of Technology, Cambridge.

Since 1988, he has been as Assistant Professor at the Sloan School of Management at MIT. He teaches courses in product development, operations management, and the management of technology. His research focuses on improving product design and manufacturing practices. His current projects include developing design for manufacture techniques, organizing product development activities, improving the quality of manufacturing processes using analytical models, and controlling factory automation systems with on-line sensors.

Warren P. Seering received the Bachelor's and Master's degrees from the University of Missouri at Columbia and the Ph.D. degree from Stanford University, Stanford, CA.

He joined the faculty of the Mechanical Engineering Department at the Massachusetts Institute of Technology, Cambridge, in 1978. His areas of research interest are in performance of dynamic systems, robotics, automation, and design.